PHYSICAL REVIEW B **94**, 081106(R) (2016)

Localized and mixed valence state of Ce 4f in superconducting and ferromagnetic CeO$_{1-x}$F$_x$BiS$_2$ revealed by x-ray absorption and photoemission spectroscopy

T. Sugimoto,[1,2] D. Ootsuki,[1,2] E. Paris,[3,4] A. Iadecola,[5] M. Salome,[5] E. F. Schwier,[6] H. Iwasawa,[6] K. Shimada,[6] T. Asano,[7]
R. Higashinaka,[7] T. D. Matsuda,[7] Y. Aoki,[7] N. L. Saini,[3] and T. Mizokawa[8]
[1]*Department of Physics & Complexity Science and Engineering, University of Tokyo, 5-1-5 Kashiwanoha 277-8561, Japan*
[2]*Institute for Solid State Physics, University of Tokyo, 5-1-5 Kashiwanoha 277-8561, Japan*
[3]*Dipartimento di Fisica, Universitá di Roma "La Sapienza", Piazzale Aldo Moro 2, 00185 Roma, Italy*
[4]*Center for Life NanoScience@Sapienza, Istituto Italiano di Tecnologia, V. le Regina Elena 291, 00185 Rome, Italy*
[5]*ESRF–The European Synchrotron, 71 avenue des Martyrs, 38043 Grenoble Cedex 9, France*
[6]*Hiroshima Synchrotron Radiation Center, Hiroshima University, Hiroshima 739-0046, Japan*
[7]*Department of Physics, Tokyo Metropolitan University, Tokyo 192-0397, Japan*
[8]*Department of Applied Physics, Waseda University, Tokyo 169-8555, Japan*

(Received 29 March 2016; revised manuscript received 28 July 2016; published 17 August 2016)

We have performed Ce L_3-edge x-ray absorption spectroscopy (XAS) and Ce 4d-4f resonant photoemission spectroscopy (PES) on single crystals of CeO$_{1-x}$F$_x$BiS$_2$ for $x = 0.0$ and 0.5 in order to investigate the Ce 4f electronic states. In Ce L_3-edge XAS, a mixed valence of Ce was found in the $x = 0.0$ sample, and F doping suppressed it, which is consistent with the results on polycrystalline samples. As for resonant PES, we found that the Ce 4f electrons in both $x = 0.0$ and 0.5 systems respectively formed a flat band at 1.0 and 1.4 eV below the Fermi level and there was no contribution to the Fermi surfaces. Interestingly, Ce valence in CeOBiS$_2$ deviates from Ce^{3+} even though Ce 4f electrons are localized, indicating the Ce valence is not in a typical valence fluctuation regime. We assume that localized Ce 4f in CeOBiS$_2$ is mixed with unoccupied Bi 6p_z, which is consistent with a previous local structural study. Based on the analysis of the Ce L_3-edge XAS spectra using Anderson's impurity model calculation, we found that the transfer integral becomes smaller, increasing the number of Ce 4f electrons upon the F substitution for O.

DOI: 10.1103/PhysRevB.94.081106

Since the discovery of superconductivity in the BiS$_2$ system by Mizuguchi *et al.* [1], the electronic and lattice structures of various BiS$_2$-based superconductors have been attracting great interest, including REO$_{1-x}$F$_x$BiS$_2$ (RE: rare-earth elements) [2–16]. In a typical REO$_{1-x}$F$_x$BiS$_2$ system, a REO$_{1-x}$F$_x$ block layer and BiS$_2$ layer are alternatively stacked, and F substitution for O is considered as electron doping to the electronically active BiS plane [17], whereas it has been found continuously that the actual carrier concentration is always smaller than its nominal value [18–20]. Among the various REO$_{1-x}$F$_x$BiS$_2$ compounds, CeO$_{1-x}$F$_x$BiS$_2$ is very unique in that superconductivity in the BiS$_2$ layer and ferromagnetism in the CeO$_{1-x}$F$_x$ layer coexist for $x > 0.4$ [21]. Meanwhile, an x-ray absorption spectroscopy (XAS) study on CeO$_{1-x}$F$_x$BiS$_2$ has revealed that the Ce valence is intermediate (valence fluctuation) and Ce 4f states may contribute to the Fermi surfaces for $x < 0.4$, and that F doping makes the system crossover from a valence fluctuation regime to a Kondo-like regime [22]. However, from dc susceptibility measurements on CeOBiS$_2$, Ce 4f electrons are found to be in a well-localized state [23], which is inconsistent with the XAS results. In order to identify the role of Ce 4f electrons, we have investigated the electronic states of Ce 4f in CeO$_{1-x}$F$_x$BiS$_2$ using Ce L_3-edge XAS and Ce 4d-4f resonant angle-resolved photoemission spectroscopy (ARPES).

High-quality single crystals of CeOBiS$_2$ and CeO$_{0.5}$F$_{0.5}$BiS$_2$ have been prepared by the CsCl flux method [23]. As for the stoichiometry of the $x = 0.5$ sample, the observed lattice constant $c = 13.443$ Å is reasonable compared with previous studies on the Ce(O,F)BiS$_2$ system [21,24]. The Ce L_3 XAS measurements were performed at ID21, ESRF. At ID21, a double-crystal fixed-exit Si(111) monochromator (Kohzu, Japan) was used for the energy scans. The beam was focused down to a microprobe by a Kirkpatrick-Baez mirror system. All the spectra were taken in the fluorescence yield mode, and the fluorescence detector was a 10 mm^2 silicon drift diode (Röntec, Germany). Acquisition was performed at low temperature using a liquid nitrogen cryostat. The resonant ARPES measurements with linearly polarized photons were performed at the undulator beamline BL-1 of HSRC, Hiroshima University. The end station was equipped with a Scienta Omicron R4000 analyzer. The photon energy was set to be 30–130 eV. We cleaved the single crystalline sample *in situ* under ultrahigh vacuum ($< 1 \times 10^{-10}$ Torr) to obtain a clean (001) surface. The total energy resolutions were measured to be 21 and 103 meV at $h\nu = 30$ and 120 eV, respectively. The angular resolution was 0.7°, corresponding to 0.032 Å^{-1} for 30 eV and 0.067 Å^{-1} for 130 eV in momentum space. All the ARPES measurements were performed at 50 K with p-polarization geometry.

Figures 1(a) and 1(b) show the real space 50 μm × 50 μm images of XAS intensities at the Ce L_3 edge (5.732 keV) on CeOBiS$_2$ and CeO$_{0.5}$F$_{0.5}$BiS$_2$, respectively. From these images, one can see that the Ce 4f electronic states are spatially homogeneous in this scale. We also confirmed that the spectral shape at the dark spot is the same as that of the bright spot, indicating that the intensity modulation is not derived from electronic inhomogeneity.

Figure 1(c) shows the normalized Ce L_3-edge XAS spectra of CeOBiS$_2$ and CeO$_{0.5}$F$_{0.5}$BiS$_2$. The spectra were normalized

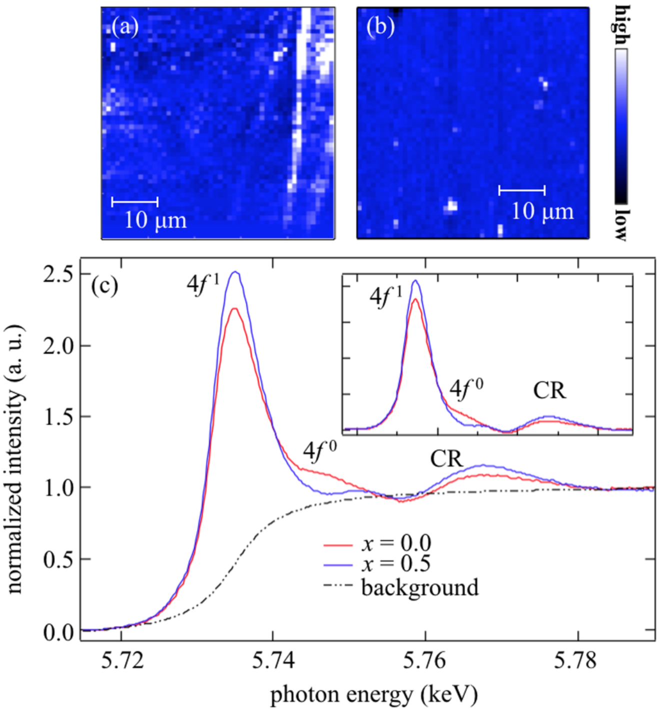

FIG. 1. (a) Real space image of micro x-ray absorption near edge structure (μXANES) at the Ce L_3 edge (5.732 keV) on CeOBiS$_2$ and (b) on CeO$_{0.5}$F$_{0.5}$BiS$_2$. (c) Normalized XAS spectra of CeOBiS$_2$ and CeO$_{0.5}$F$_{0.5}$BiS$_2$. The background (arctangent function) is denoted by the dotted-dashed line. The spectra after background subtraction are also shown in the inset.

with respect to the atomic absorption estimated by a linear fit to the high energy part of the spectra, as used in the earlier study [22]. The background (arctangent function) is shown by the dotted-dashed line. The background-subtracted spectra are also shown in the inset with the same energy and intensity scales. Three main structures around 5.732, 5.745, and 5.768 keV can be identified in the Ce L_3-edge XAS spectra. The first (second) feature is the transition from Ce $2p$ to Ce $5d$ mixed with a $4f^1$ ($4f^0$) final state [25–28]. The coexistence of the first and second peaks suggests that Ce^{3+} and Ce^{4+} coexist in the system. Here, the spatially homogeneous XAS map indicates that the observed f^0/f^1 mixed valence is not due to CeO$_2$ impurities but is an intrinsic physics. The third feature is the so-called continuum resonance (CR) derived from Ce-Bi scattering, and reflects the Ce-Bi bond length [22]. In addition to the three main features, there is a weak structure around 5.75 keV. This is the typical structure of a layered rare-earth system, and its intensity is sensitive to the O/F atomic order/disorder in the Ce(O,F) layer [22]. All the XAS results are quantitative consistent with the previous Ce L_3-edge XAS results of polycrystalline CeO$_{1-x}$F$_x$BiS$_2$ [22]. However, an inconsistency with the dc susceptibility measurement still remains; in CeOBiS$_2$, the XAS result suggests that the Ce $4f$ electrons are valence fluctuating whereas the dc susceptibility measurement found Ce $4f$ to be well localized. We have performed Ce $4d$-$4f$ resonant ARPES on the CeOBiS$_2$ and CeO$_{0.5}$F$_{0.5}$BiS$_2$ single crystals in order to investigate the Ce $4f$ electronic states and specify the orbitals mixing with Ce $4f$ in CeOBiS$_2$.

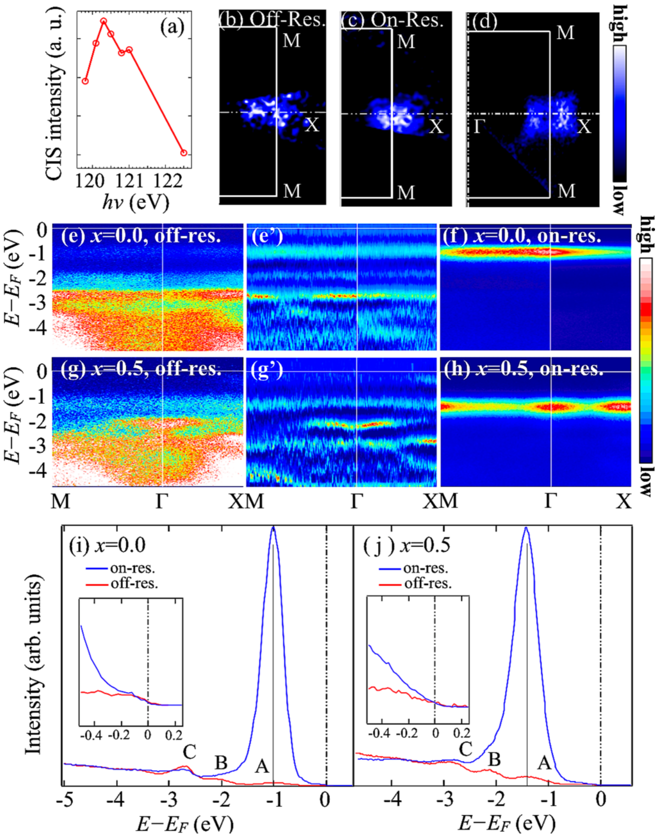

FIG. 2. (a) CIS plot of CeO$_{0.5}$F$_{0.5}$BiS$_2$. Fermi surfaces of CeO$_{0.5}$F$_{0.5}$BiS$_2$ taken (b) at 120.3 eV on resonance, (c) at 115.4 eV off resonance, and (d) at 30 eV. The ARPES intensities are integrated within ±50 meV with respect to E_F. (e) Cut along M-Γ-X with off-resonant $h\nu$ and (e′) its second derivative, (f) cut with on-resonant photon energy, (i) EDCs integrated along M-Γ-X for both off- and on-resonant $h\nu$, and the inset shows the expanded view near E_F on CeOBiS$_2$. (g), (g′), (h), and (j) are the same as (e), (e′), (d), and (i) but on CeO$_{0.5}$F$_{0.5}$BiS$_2$.

Figure 2(a) shows a constant initial state (CIS) plot with respect to the photon energy at the Ce $4f$ peak of CeO$_{0.5}$F$_{0.5}$BiS$_2$ normalized by the photon flux, which determines the Ce $4d$-$4f$ on-resonant photon energy of the system as 120.3 eV. Figures 2(b) and 2(c) show the Fermi surface maps of CeO$_{0.5}$F$_{0.5}$BiS$_2$ at 115.4 eV off resonance and 120.3 eV on resonance. They are obtained by rotating the azimuthal angle with respect to the crystallographic c axis of the sample. Since there are no considerable changes in the Fermi surfaces with the on- and off-resonant photon energies, the Ce $4f$ electrons are not employed as part of the Fermi surfaces. The Fermi surfaces measured at 30 eV are shown in Fig. 2(d), whose Luttinger volume is 0.22 whereas the nominal x is 0.5 (see details in Ref. [20]).

Figures 2(e) and 2(f) [Figs. 2(g) and 2(h)] show the ARPES data taken at 115.4 eV (off resonance) and 120.3 eV (on resonance), respectively, for CeOBiS$_2$ (for CeO$_{0.5}$F$_{0.5}$BiS$_2$) along M-Γ-X. Figures 2(i) and 2(j) respectively show the energy distribution curves (EDCs) integrated along M-Γ-X taken for CeOBiS$_2$ and CeO$_{0.5}$F$_{0.5}$BiS$_2$ at on- and off-resonant photon energies, and the inset shows the expansion near E_F. One can see from the EDCs [Figs. 2(i) and 2(j)] that the structures A, B, and C of $\mathrm{CeO_{0.5}F_{0.5}BiS_2}$ are roughly shifted to a higher binding energy by 0.4 eV due to electron doping compared with those of $\mathrm{CeOBiS_2}$, but one can also see there is a slight band dependence of the shifts, which could be due to local atomic structural changes [29]. The on-resonance spectra are dominated by the partial density of states (DOS) of Ce 4f due to the resonant enhancement. If the system is in a conventional valence fluctuating regime, the on-resonant spectrum considerably enhances two features: at approximately 0 eV (f^0 component) due to a strong c–f hybridization and at -1.0 eV (f^1 component) in $\mathrm{CeOBiS_2}$ [at 0 eV (f^0) and at -1.4 eV (f^1) in $\mathrm{CeO_{0.5}F_{0.5}BiS_2}$] with respect to E_F. On the other hand, if the system is in a Kondo-like regime, the on-resonant enhancement can be seen in one feature: at -1.0 eV in $\mathrm{CeOBiS_2}$ (at -1.4 eV in $\mathrm{CeO_{0.5}F_{0.5}BiS_2}$) with respect to E_F, which is the f^1 component [30].

In $\mathrm{CeO_{0.5}F_{0.5}BiS_2}$, the Bi 6$p$ Fermi pocket around the X point is observed in both the on- and off-resonance data. The valence band below -1 eV can be assigned to the Bi 6s, S 3p, and Ce 4f bands. When the photon energy is tuned to the Ce 4d-4f absorption energy (120.7 eV), the flat band located at -1.4 eV is considerably enhanced. The resonant ARPES results show that the Ce 4f band is located between the Bi 6p conduction band and the Bi 6s/S 3p valence band, and that there is no appreciable Ce 4f spectral weight at E_F. Namely, the results indicate that the Ce 4f electrons are basically localized (Kondo-like regime), do not contribute to the Fermi pockets around X, and their valence should be 3+. This result on $\mathrm{CeO_{0.5}F_{0.5}BiS_2}$ is consistent with the bulk sensitive Ce L_3-edge XAS result where $\mathrm{CeOBiS_2}$ falls in the valence fluctuation regime and gradually changes to the Kondo-like regime with F substitution for O [22]. The superexchange or Ruderman-Kittel-Kasuya-Yosida (RKKY) interaction between the localized Ce 4f moments is derived from Ce 4f-S 3p hybridization.

On the other hand, in $\mathrm{CeOBiS_2}$, we found that the Ce 4f line shape is very similar to that of $\mathrm{CeO_{0.5}F_{0.5}BiS_2}$, as shown in Figs. 2(i) and 2(j), and is different from what one expected for valence fluctuating systems. In typical valence fluctuating systems such as $\mathrm{CeRu_2}$, the Ce 4f band is strongly hybridized with the conduction band such as Ru 4d and is well reproduced by local density approximation (LDA) band calculations. The observed Ce 4f band of $\mathrm{CeOBiS_2}$ has a very flat dispersion and does not agree with the LDA band calculation [20]. Here, we speculate that the Ce 4f electrons in $\mathrm{CeOBiS_2}$ are mixed with the unoccupied Bi 6p_z. From the crystal structure, the nearest ion for Ce is oxygen, but the oxygen band is located far from E_F by 3–4 eV and therefore is hard to hybridize with Ce 4f. The other candidate for the mixing partner of Ce 4f is unoccupied Bi 6p_z through the out-of-plane S. Since the Bi 6p_z orbitals do not contribute to the Fermi surfaces, one electron in the Ce 4f orbitals should be completely transferred to the Bi 6p_z orbitals in order to obtain the f^0 component in the Ce L_3 XAS. However, if the electron transfer from the Bi 6s orbitals to the Ce 4f orbitals is included, the mixture of the f^1 and f^0 states becomes possible and the Ce L_3 XAS result would be explained. Note that Ce 4f-Bi 6p_z hybridization does not necessarily lead to a metallic state. It provides a mixed valence state given by the linear combination of $|4f^1\rangle$ and $|4f^0\,L^1\rangle$, where L is Bi 6p_z. This state can be localized if the overlap between the neighboring Bi 6p_z states is sufficiently small compared with the intersite Coulomb repulsive energy. Even if the overlap is not small enough for the localization due to the pure Coulomb interaction, the combination of the Coulomb interaction and the atomic disorder [29] can provide an insulating ground state, possibly a sort of charge glass of Bi 6p_z electrons. Moreover, this hybridization may impede the ferromagnetic order in the Ce(O,F) layer.

In order to examine this possibility, we have performed Anderson's impurity model (AIM) calculation on Ce L_3-edge XAS results under the condition that the Ce 4f is mixing with the unoccupied Bi 6p_z and the occupied Bi 6s. The model Hamiltonian is given by the standard Anderson Hamiltonian including the Ce 4f/5d electrons, the conduction-band electrons, and the Ce 2p core-level electrons.

$$\begin{aligned}\mathscr{H}_{\mathrm{A}} = {} & \sum_k \varepsilon_k c_k^\dagger c_k + \varepsilon_f \sum_m f_m^\dagger f_m + U_f \sum_{m'>m} f_{m'}^\dagger f_{m'} f_m^\dagger f_m \\ & + n_{\mathrm{c}}\varepsilon_{\mathrm{c}} + (1-n_{\mathrm{c}}) Q_f \sum_m f_m^\dagger f_m \\ & + \sum_{mk} (V_{mk} c_k^\dagger f_m + V_{mk}^* f_m^\dagger c_k) \\ & + \varepsilon_d \sum_m d_m^\dagger d_m + U_{fd} \sum_{m'>m} f_{m'}^\dagger f_{m'} d_m^\dagger d_m \\ & + (1-n_{\mathrm{c}}) Q_d \sum_m d_m^\dagger d_m . \end{aligned} \tag{1}$$

Here, $f_m^\dagger$ ($d_m^\dagger$) are the creation operators for the Ce 4f (5d) electrons with the orbital notation m, and $c_k^\dagger$ are creation operators for Bloch electrons in the Bi 6p_z and Bi 6s bands with wave vector $\boldsymbol{k}$. The parameters U_f and Q_f (Q_d) are the on-site repulsive Coulomb interaction between the Ce 4f electrons and the attractive Coulomb interaction between the Ce 4f (5d) electron and the Ce 2p core hole, and U_{fd} is the on-site repulsive Coulomb interaction between the Ce 4f and Ce 5d electrons. Note that the notations m and k include spin. The parameter V describes the transfer integral between the Ce 4f and conduction-band electrons, ε_f (ε_d) is the energy level of Ce 4f (5d) electrons relative to the Fermi level, and $\varepsilon_{\mathrm{c}}/n_{\mathrm{c}}$ represent the energy/number of the Ce 2p core-level electron.

In the Ce L_3-edge XAS process, the absorption occurs from the Ce 2p core level to the Ce 5d unoccupied states mixed with the Ce 4f states. In the framework of Anderson's impurity model, the initial state can be simply given by

$$|\psi_i\rangle = \alpha|4f^0\,L^1\rangle + \beta|4f^1\rangle + \gamma|4f^2\,\underline{L}^1\rangle, \tag{2}$$

where L and $\underline{L}$ denote a Bi 6p_z electron and Bi 6s hole, respectively. The final states are given by

$$\begin{aligned}|\psi_f\rangle = {} & \alpha'|\underline{c}\,4f^0\,L^1\,5d^1\rangle + \beta'|\underline{c}\,4f^1\,5d^1\rangle \\ & + \gamma'|\underline{c}\,4f^2\,\underline{L}^1\,5d^1\rangle,\end{aligned} \tag{3}$$

where $\underline{c}$ denotes the Ce 2p core hole. Using α, β, γ, α', β', and γ', the spectral weight is given by $|\alpha\alpha' + \beta\beta' + \gamma\gamma'|^2$. The

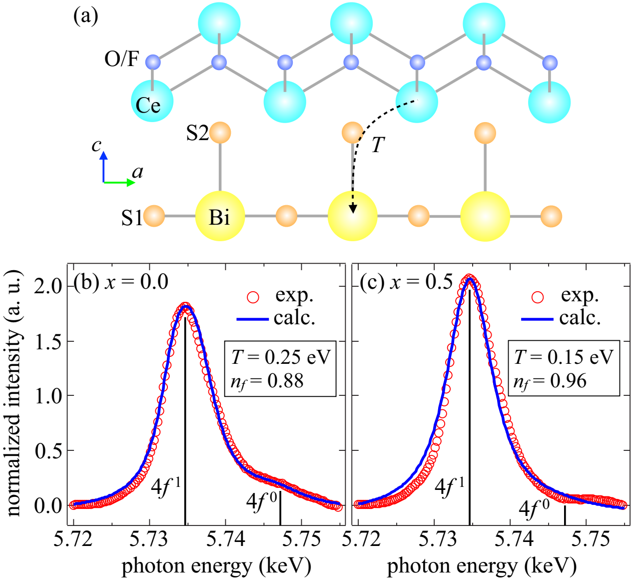

FIG. 3. (a) Schematic diagram of the effective transfer integral T. Ce L_3-edge XAS experimental results on single crystal $CeO_{1-x}F_xBiS_2$ and corresponding impurity model calculations at (a) $x = 0.0$ and (b) $x = 0.5$. The energy positions of $4f^1$ and $4f^0$ are shown by vertical lines. The effective transfer integral (T) and number of Ce $4f$ electrons (n_f) estimated by Anderson's impurity model calculation are also shown here.

energy of the $|\underline{c}\,4f^0\,L^1\,5d^1\rangle$ state is given by $\varepsilon_d - Q_d$, that of the $|\underline{c}\,4f^1\,5d^1\rangle$ is given by $\varepsilon_f + \varepsilon_d - Q_f - Q_d + U_{fd}$, and that of $|\underline{c}\,4f^2\,\underline{L}^1\,5d^1\rangle$ is given by $2\varepsilon_f + \varepsilon_d - 2Q_f - Q_d + U_f + 2U_{fd}$.

The parameters U_{fd} and Q_d are neglected in the present analysis because they are substantially small compared with the other parameters. Since ε_f can be determined by the Ce $4d$-$4f$ resonant ARPES results and Q_f is fixed at $U_f/0.8$ [31,32], the present analysis includes two free parameters, U_f and T, where the effective transfer integral $T = \sqrt{\sum_{mk} |V_{mk}|^2}/\sqrt{N}$ with $N = 14$ [see Fig. 3(a)] represents the off-diagonal term. For simplicity, the effective transfer integral is the same for the Bi $6p_z$ and $6s$ orbitals.

Considering the local structural changes of Ce, S2 [see Fig. 3(a)], and Bi due to the F doping [29], the parameter T should be the only adjustable parameter to reproduce the XAS spectra. Therefore, the parameter U_f is fixed at 7.8 eV for all the calculations. We can reproduce the $4f^1$ and $4f^0$ structures of the XAS spectra, indicating that the scenario above could be possible. The results are shown in Figs. 3(b) and 3(c) for $x = 0.0$ and 0.5, respectively, and the energy positions of the $4f^1$ and $4f^0$ structures are also shown here. The circles and solid lines are respectively the experimental and calculated results, and the evaluated T and number of Ce $4f$ electrons (n_f) are also shown in Fig. 3. The parameter T changes from 0.25 to 0.15 eV when the F concentration x goes from 0.0 to 0.5. The number n_f is calculated as 0.88 and 0.96 for $x = 0.0$ and 0.5, respectively. The present results are qualitatively consistent with the previous impurity model calculations on a polycrystalline system [33]. Moreover, this is also consistent with the thermodynamical quantities because Higashinaka *et al.* reported that the amount of Ce^{3+} ($4f^1$ state) in $CeOBiS_2$ is 10% lower than expected [23], and the impurity model calculation shows $n_f = 0.88$.

Our scenario could explain the XAS and resonant ARPES results naturally with support from the AIM calculation; the unoccupied Bi $6p_z$ states partially trap Ce $4f$ electrons and form a sort of charge glass state due to the strong atomic disorder of the BiS plane. It is expected that the electrons in the Bi $6p_z$ state are randomly distributed in real space and appear as a broad feature in the ARPES spectra. Therefore, it would be rather difficult to identify the Bi $6p_z$ state from a comparison between the photoemission results and some calculations considering the atomic disorder in the BiS plane. Note that our argument is not sensitive to the value of x itself as long as the system shows superconductivity even though the uncertainty of $x = 0.5$ crystal still remains here.

In summary, we have combined Ce L_3-edge XAS, Ce $4d$-$4f$ resonant ARPES, and AIM calculations on single crystals of $CeO_{1-x}F_xBiS_2$ for $x = 0.0$ and 0.5 in order to investigate the electronic states of Ce $4f$ electrons. The XAS found that the $x = 0.0$ sample is in a mixed valence state that is suppressed by F doping, which is consistent with a previous study [22]. The resonant ARPES found that the Ce $4f$ electrons in both $x = 0.0$ and 0.5 systems are essentially localized and there is no contribution to the Fermi surfaces. We assume that the localized Ce $4f$ in $CeOBiS_2$ is mixed with the unoccupied Bi $6p_z$ instead of Bi $6p_x/6p_y$. This scenario is consistent with a previous local structural study. The AIM calculation not only supports the scenario, but also is consistent with the thermodynamical experiments [23]. The hybridization of Ce $4f$ and Bi $6p_z$ may impede the ferromagnetic order in the Ce(O,F) layer.

The authors are grateful to M. Zheng and Y. Kojima for their support during the experimental run at BL-1, Hiroshima Synchrotron Radiation Center. T.S. and D.O. acknowledge support from a JSPS Research Fellowship for Young Scientists. This work is partly supported by JSPS KAKENHI (Grants No. 15H03693 and No. 25400356). E.F.S. acknowledges financial support from a JSPS postdoctoral fellowship for overseas researchers as well as the Alexander von Humboldt Foundation (Grant No. P13783). The synchrotron radiation experiments have been done with the approval of Hiroshima Synchrotron Radiation Center (Proposal No. 14-B-24).

---

[1] Y. Mizuguchi, H. Fujihisa, Y. Gotoh, K. Suzuki, H. Usui, K. Kuroki, S. Demura, Y. Takano, H. Izawa, and O. Miura, Phys. Rev. B **86**, 220510(R) (2012).

[2] S. K. Singh, A. Kumar, B. Gahtori, G. Sharma, S. Patnaik, and V. P. S. Awana, J. Am. Chem. Soc. **134**, 16504 (2012).

[3] B. Li, Z. W. Xing, and G. Q. Huang, Europhys. Lett. **101**, 47002 (2013).

[4] K. Deguchi, Y. Mizuguchi, S. Demura, H. Hara, T. Watanabe, S. J. Denholme, M. Fujioka, H. Okazaki, T. Ozaki, H. Takeya, T. Yamaguchi, O. Miura, and Y. Takano, Europhys. Lett. **101**, 17004 (2013).

[5] H. Kotegawa, Y. Tomita, H. Tou, H. Izawa, Y. Mizuguchi, O. Miura, S. Demura, K. Deguchi, and Y. Takano, J. Phys. Soc. Jpn. **81**, 103702 (2012).

[6] S. Demura, Y. Mizuguchi, K. Deguchi, H. Okazaki, H. Hara, T. Watanabe, S. J. Denholme, M. Fujioka, T. Ozaki, H. Fujihisa, Y. Gotoh, O. Miura, T. Yamaguchi, H. Takeya, and Y. Takano, J. Phys. Soc. Jpn. **82**, 033708 (2013).

[7] V. P. S. Awana, A. Kumar, R. Jha, S. K. Singh, A. Pal, Shruti, J. Saha, and S. Patnaik, Solid State Commun. **157**, 21 (2013).

[8] R. Jha, A. Kumar, S. K. Singh, and V. P. S. Awana, J. Appl. Phys. **113**, 056102 (2013).

[9] J. Xing, S. Li, X. Ding, H. Yang, and H.-H. Wen, Phys. Rev. B **86**, 214518 (2012).

[10] D. Yazici, K. Huang, B. D. White, A. H. Chang, A. J. Friedman, and M. B. Maple, Philos. Mag. **93**, 673 (2012).

[11] D. Yazici, K. Huang, B. D. White, I. Jeon, V. W. Burnett, A. J. Friedman, I. K. Lum, M. Nallaiyan, S. Spagna, and M. B. Maple, Phys. Rev. B **87**, 174512 (2013).

[12] T. Yildirim, Phys. Rev. B **87**, 020506(R) (2013).

[13] Y. Liang, X. Wu, W-F. Tsai, and J. Hu, Front. Phys. **9**, 194 (2014).

[14] X. Wan, H. C. Ding, S. Y. Savrasov, and C. G. Duan, Phys. Rev. B **87**, 115124 (2013).

[15] J. Lee, M. B. Stone, A. Huq, T. Yildirium *et al.*, Phys. Rev. B **87**, 205134(R) (2013).

[16] G. Lamura, T. Shiroka, P. Bonfá, S. Sanna, R. De Renzi, C. Baines, H. Luetkens, J. Kajitani, Y. Mizuguchi, O. Miura, K. Deguchi, S. Demura, Y. Takano, and M. Putti, Phys. Rev. B **88**, 180509(R) (2013).

[17] C. Morice, E. Artacho, S. E. Dutton, H.-J. Kim, and S. S. Saxena, J. Phys.: Condens. Matter **28**, 345504 (2016).

[18] Z. R. Ye, H. F. Yang, D. W. Shen, J. Jiang, X. H. Niu, D. L. Feng, Y. P. Du, X. G. Wan, J. Z. Liu, X. Y. Zhu, H. H. Wen, and M. H. Jiang, Phys. Rev. B **90**, 045116 (2014).

[19] L. K. Zeng, X. B. Wang, J. Ma, P. Richard, S. M. Nie, H. M. Weng, N. L. Wang, Z. Wang, T. Qian, and H. Ding, Phys. Rev. B **90**, 054512 (2014).

[20] T. Sugimoto, D. Ootsuki, C. Morice, E. Artacho, S. S. Saxena, E. F. Schwier, M. Zheng, Y. Kojima, H. Iwasawa, K. Shimada, M. Arita, H. Namatame, M. Taniguchi, M. Takahashi, N. L. Saini, T. Asano, R. Higashinaka, T. D. Matsuda, Y. Aoki, and T. Mizokawa, Phys. Rev. B **92**, 041113(R) (2015).

[21] S. Demura, K. Deguchi, Y. Mizuguchi, K. Sato, R. Honjyo, A. Yamashita, T. Yamaki, H. Hara, T. Watanabe, S. J. Denholme, M. Fujioka, H. Okazaki, T. Ozaki, O. Miura, T. Yamaguchi, H. Takeya, and Y. Takano, J. Phys. Soc. Jpn. **84**, 024709 (2015).

[22] T. Sugimoto, B. Joseph, E. Paris, A. Iadecola, T. Mizokawa, S. Demura, Y. Mizuguchi, Y. Takano, and N. L. Saini, Phys. Rev. B **89**, 201117(R) (2014).

[23] R. Higashinaka, T. Asano, T. Nakashima, K. Fushiya, Y. Mizuguchi, O. Miura, T. D. Matsuda, and Y. Aoki, J. Phys. Soc. Jpn. **84**, 023702 (2015).

[24] M. Nagao, A. Miura, S. Demura, K. Deguchi, S. Watauchi, T. Takei, Y. Takano, N. Kumada, and I. Tanaka, Solid State Commun. **178**, 33 (2014).

[25] B. T. Thole, G. van der Laan, J. C. Fuggle, G. A. Sawatzky, R. C. Karnatak, and J.-M. Esteva, Phys. Rev. B **32**, 5107 (1985).

[26] H. Matsuyama, I. Harada, and A. Kotani, J. Phys. Soc. Jpn. **66**, 337 (1997).

[27] A. Kotani, K. O. Kvashnina, P. Glatzel, J. C. Parlebas, and G. Schmerber, Phys. Rev. Lett. **108**, 036403 (2012).

[28] T. Kroll, F. Roth, A. Koitzsch, R. Kraus, D. R. Batchelor, J. Werner, G. Behr, B. Büchner, and M. Knupfer, New J. Phys. **11**, 025019 (2009).

[29] E. Paris, B. Joseph, A. Iadecola, T. Sugimoto, L. Olivi, S. Demura, Y. Mizuguchi, Y. Takano, T. Mizokawa, and N. L. Saini, J. Phys.: Condens. Matter **26**, 435701 (2014).

[30] O. Gunnarsson and K. Schönhammer, Phys. Rev. Lett. **50**, 604 (1983).

[31] K. Okada and A. Kotani, J. Phys. Soc. Jpn. **58**, 2578 (1989).

[32] A. E. Bocquet, T. Mizokawa, T. Saitoh, H. Namatame, and A. Fujimori, Phys. Rev. B **46**, 3771 (1992).

[33] T. Sugimoto, B. Joseph, E. Paris, A. Iadecola, T. Mizokawa, S. Demura, Y. Mizuguchi, Y. Takano, and N. L. Saini, J. Phys.: Conf. Ser. **592**, 012073 (2015).